VIP Sequential Catalysis Very Important Paper

International Edition: DOI: 10.1002/anie.201604658
German Edition: DOI: 10.1002/ange.201604658

A Metalloregulated Four-State Nanoswitch Controls Two-Step Sequential Catalysis in an Eleven-Component System

*Sudhakar Gaikwad[+], Abir Goswami[+], Soumen De, and Michael Schmittel**

Dedicated to Professor U. Lüning on the occasion of his 60th birthday

Abstract: *The nanomechanical switch **1** with its three orthogonal binding motifs—the zinc(II) porphyrin, azaterpyridine, and shielded phenanthroline binding station—is quantitatively and reversibly toggled back and forth between four different switching states by means of addition and removal of appropriate metal-ion inputs. Two of the four switching stages are able to initiate catalytic transformations (ON1, ON2), while the two others shut down any reaction (OFF1, OFF2). Thus, in a cyclic four-state switching process the sequential transformation* $\mathbf{A}+\mathbf{B}+\mathbf{C}\rightarrow\mathbf{AB}+\mathbf{C}\rightarrow\mathbf{ABC}$ *can be controlled, which proceeds stepwise along the switching states OFF1→ON1 (click reaction:* $\mathbf{A}+\mathbf{B}\rightarrow\mathbf{AB}$*)→OFF2→ON2 (Michael addition:* $\mathbf{AB}+\mathbf{C}\rightarrow\mathbf{ABC}$*)→OFF1. Two consecutive cycles of the sequential catalysis were realized without loss in activity in a reaction system with eleven different components.*

Metalloregulated switches play an important role in many physiological processes with transition-metal ions acting as cofactors or as coordination centers for large-amplitude toggling.[1] Owing to the key role of metals, nature has designed numerous methods for the selective transport of transition-metal ions, such as copper(I,II), iron(II),[1] across membranes into the cytoplasm and to the required protein sites. For this process, a sophisticated mechanism is used for intracellular metal-ion metabolism ("metallome").[1,2] To fathom out and develop the enormous potential of metalloregulated large-amplitude switching[3] also outside of the biosphere, we have focused in our research on metal-ion-controlled nanoswitches with a particular emphasis on the allosteric control[4] of catalytic processes. Although switchable catalysis has become a topical issue in the last few years,[5] most of the switches involved operate on light[6] and pH control,[7] whereas highly selective chemical inputs (addition of ligands/anions[8] or metal ions)[9,10] for controlling catalysis are rare. While light is a common preferred choice for single switching processes,[11] variable chemical inputs are more suitable for addressing more than two switching steps. Moreover, the concentration of chemical inputs may be modulated, enabling communication between switches[12] as well as regulation and feedback control, similar to that in enzyme networks.[5c]

Inspired by nature's metal switches[1] we present herein a novel four-state nanoswitch, which is reversibly toggled back and forth between all switching states. Moreover, the nanoswitch toggles two distinct catalytic processes (a click reaction and a Michael addition) that can be applied without loss of activity over two switching cycles to the sequential transformation $\mathbf{A}+\mathbf{B}+\mathbf{C}\rightarrow\mathbf{AB}+\mathbf{C}\rightarrow\mathbf{ABC}$ requiring largely full orthogonality of a total of eleven components. Nature also uses multi-step sequential catalysis to effect transformations of supreme efficiency and selectivity toward complex biomolecules.[13]

For the four-state switch **1** we have chosen a different architecture[14] than for our previous nanoswitches that have already demonstrated their ability for ON/OFF regulation in photochemical processes[10b] as well as in organo-[10a] and transition-metal catalysis.[10c,e] Switch **1** is based on the highly versatile tetraphenylmethane scaffold equipped with three arms and three distinct terminals, a zinc(II) porphyrin (ZnPor) unit, an azaterpyridine arm that includes two functional ligands, and a shielded phenanthroline. Their exact position in the scaffold was conceived by molecular modeling so that three orthogonal binding motifs, a) an intramolecular $N_{azaterpy}\rightarrow$ZnPor linkage (in state IV), b) an intramolecular HETTAP copper complex (heteroleptic terpyridine and phenanthroline;[15] in state I), and c) an intermolecular iron(II) bisterpyridine complex (in state III), may form depending on the chosen metal ion input (Cu^+, Fe^{2+}, or none). Moreover, we hypothesized, based on previous findings,[10c] that the reaction of $[Cu(\mathbf{1})]^+$ with Fe^{2+} would afford the dimeric $[Cu_2Fe(\mathbf{1})_2]^{4+}$ (state II). Owing to the copper(I)-loaded phenanthroline, this switching state should have the potential to catalyze a click reaction, Figure 1.[10e]

Compound **1** with its three switching stations was synthesized through a multistep synthesis and unambiguously characterized by elemental analysis and the full arsenal of spectroscopic techniques. The ESI-MS spectrum displays a molecular-ion peak at m/z 1076.9 Da for $[\mathbf{1}+2H]^{2+}$, an assignment that is corroborated by the good agreement of experimental and theoretical isotopic splitting (Supporting Information, Figure S23). In the ^{1}H NMR spectrum, the pyrimidine protons a-H and b-H of the azaterpyridine unit appear as sharp signals in the aliphatic region at $\delta = 3.76$ and 2.73 ppm, respectively, confirming immersion of the pyrimidine into the shielding π-zone of the ZnPor. The $N_{azaterpy}\rightarrow$

[*] M.Sc. S. Gaikwad,[+] M.Sc. A. Goswami,[+] Dr. S. De, Prof. Dr. M. Schmittel
Center of Micro and Nanochemistry and Engineering, Organische Chemie I, Universität Siegen
Adolf-Reichwein Str. 2, 57068 Siegen (Germany)
E-mail: Schmittel@chemie.uni-siegen.de

[+] These authors contributed equally to this work.

Supporting information and the ORCID identification number(s) for the author(s) of this article can be found under http://dx.doi.org/10.1002/anie.201604658.

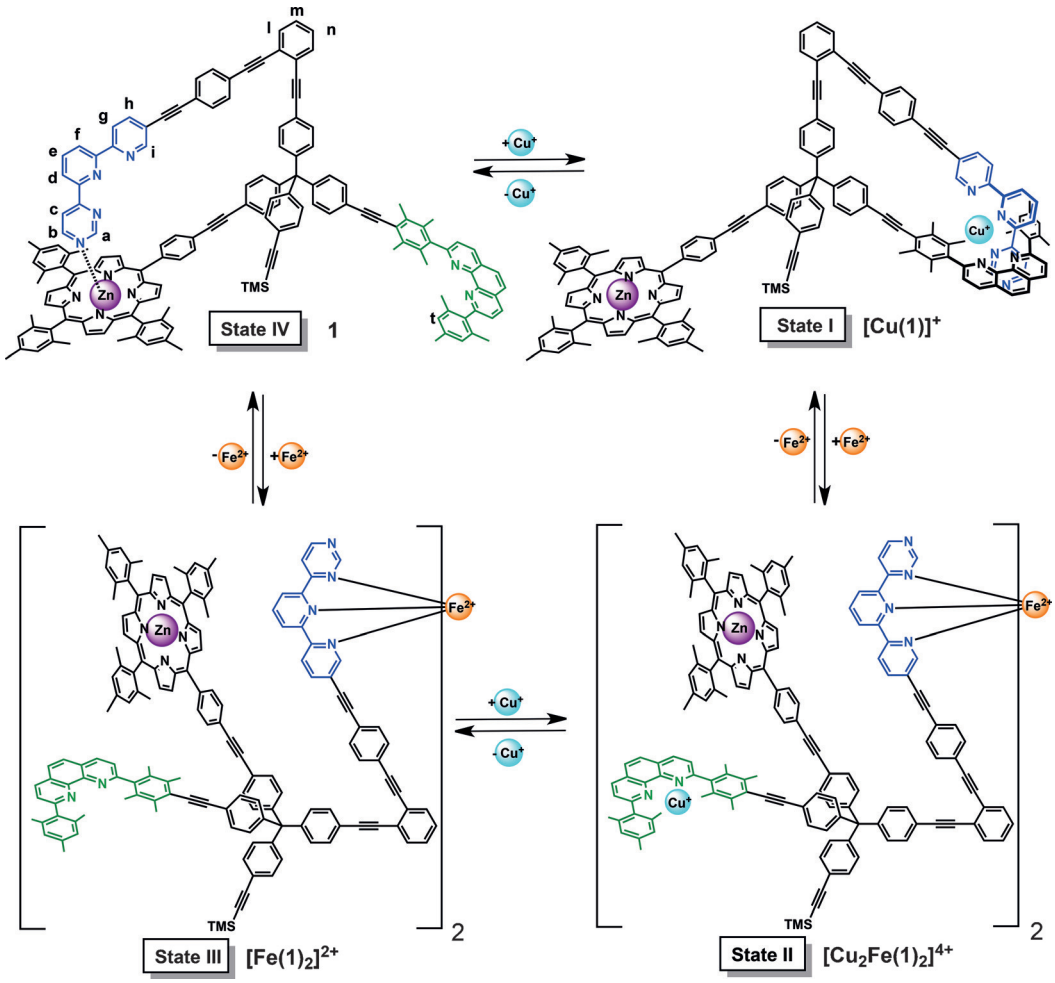

Figure 1. Nanoswitch **1** and its four switching states. TMS = trimethylsilyl.

ZnPor interaction was further validated by the UV/Vis data: the Soret band of **1** appears at $\lambda = 429$ nm, whereas the uncoordinated ZnPor unit typically displays an absorption at $\lambda = 421$ nm (Figure S27). The 8 nm shift is well documented for related pyridine-coordinated zinc(II) porphyrin systems.[10a,b] The $N_{azaterpy}$→ZnPor coordination is clearly intramolecular as indicated by the concentration independence of the chemical shifts. Thus, the UV/Vis absorption of the Q-band stays constant at $\lambda = 562$ nm over $c = 10^{-6}$ to 10^{-4} M (Figure S28). These results show that nanoswitch **1** is self-locked at the $N_{azaterpy}$→ZnPor linkage.

Initially, we prepared each of the switching states I, II, and III individually in analytically pure form. Different from **1** (state IV), the other switching states I–III should be able to inhibit catalytically active amines, such as piperidine (**2**), by strong binding at the free ZnPor unit,[10a] an important prerequisite for controlling catalysis (see below). First, the intramolecular complex $[Cu(\mathbf{1})]^+$ (state I) was prepared by adding one equivalent of $[Cu(CH_3CN)_4]PF_6$ to nanoswitch **1** (= state IV) in [D$_2$]-dichloromethane. The switching arm has to move 2.5 nm from the zinc(II) to the copper(I) center. As anticipated, the intermolecular complex $[Fe(\mathbf{1})_2]^{2+}$ (state III) was afforded quantitatively from switch **1** by addition of 0.5 equivalents of $Fe(BF_4)_2$ (Figure S8), again upon cleavage of the $N_{azaterpy}$→ZnPor linkage. The heterodimetallic complex $[Cu_2Fe(\mathbf{1})_2]^{4+}$ (state II) was prepared from both possible precursors, either from $[Cu(\mathbf{1})]^+$ (state I) by addition of 0.5 equivalents of $Fe(BF_4)_2$ or from $[Fe(\mathbf{1})_2]^{2+}$ (state III) by adding one equivalent of $[Cu(CH_3CN)_4][B(C_6F_5)_4]$ (relative to **1**). The identity and quantitative formation of switching states I–III were unambiguously established by ^{1}H NMR, ^{1}H-^{1}H COSY, and UV/Vis spectroscopic data, and ESI-MS (for complete data, see Supporting Information) as well as by elemental analysis. Some of the diagnostic changes along the switching states IV→I→II→III are highlighted in Table 1. For instance, the UV/Vis data unambiguously show that the $N_{azaterpy}$→ZnPor linkage is only present in **1** (state IV) while the ^{1}H NMR downfield shift at the azaterpyridine unit (d,f-H) indicate that the iron(II) bisterpyridine complex is realized in both switching states II and III. The loading of both phenanthroline stations with copper(I) ions in $[Cu_2Fe(\mathbf{1})_2]^{4+}$ (state II) becomes apparent from the downfield shift of protons 5,6-H when going from state III→II. Besides, the ESI-MS displays a diagnostic signal (100 %) for the complex $[Cu_2Fe(\mathbf{1})_2]^{4+}$ (Figure S26).

Table 1: Selected data of switching states I–IV.

State	UV/Vis[a] /nm	Phen[b,c]		Azaterpyridine[b]			
		t-H	5,6-H	a-H	d-H	f-H	i-H
IV	429/562	6.96	7.91	3.76	7.38	7.36	8.68
I	421/549	6.30	7.96	7.39	8.10	7.95	7.88
II	–/549	6.95	8.08	7.26	8.86	8.67	6.90
III	–/549	6.91	7.91	7.24	8.98	8.81	7.02

[a] Absorption maxima. [b] ^{1}H NMR shifts in ppm. [c] Phenanthroline. For complete ^{1}H NMR data, see Supporting Information.

Next we investigated the reversibility of toggling between selected states. Addition of $[Cu(CH_3CN)_4]PF_6$ to **1** provided complex $[Cu(\mathbf{1})]^+$, whose low binding constant ($\log K = 7.42 \pm$

0.07) reflects the parallel rupture of the $N_{azaterpy}$→ZnPor interaction (Figure S48). Addition of one equivalent of cyclam (**3**) to a solution of $[Cu(\mathbf{1})]^+$ fully restored **1**, as seen from protons a-H and t-H returning to their original positions at $\delta = 3.76$ and 6.96 ppm, respectively. Further insights were obtained from a UV/Vis titration of $[Cu(\mathbf{1})]^+$ (1×10^{-4} M) against **3** (2.5×10^{-3} M) showing that the Q-band returned from $\lambda = 549$ to 562 nm after addition of one equivalent of cyclam (Figure S30). Thus the UV/Vis and ^{1}H NMR spectroscopic studies confirmed quantitative and reversible switching between states IV and I over three cycles (Figure S11).

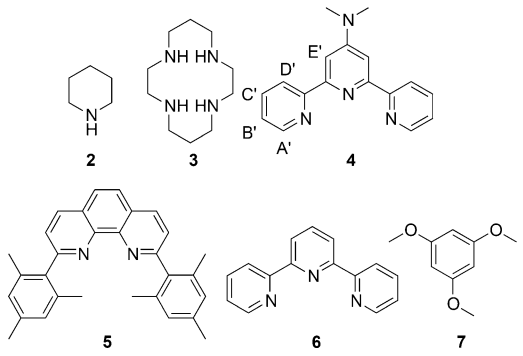

Thereafter, reversible toggling between nanoswitch **1** (state IV) and $[Fe(\mathbf{1})_2]^{2+}$ (state III) was evaluated. After addition of 0.50 equivalents of $Fe(BF_4)_2$ to **1**, the azaterpyridine protons a-H, d-H, and f-H shifted from $\delta = 3.76$, 7.38, and 7.36 ppm to 7.24, 8.98, and 8.81 ppm, respectively. The concomitant unlocking of the azaterpyridine arm at the ZnPor binding site was additionally corroborated by a UV/Vis titration of switch **1** (1×10^{-4} M) against $Fe(BF_4)_2$ (2.75×10^{-3} M) with the Q band shifting from $\lambda = 562$ to 549 nm upon addition of 0.50 equivalents of Fe^{2+}. This resulted in $\log K = 10.06 \pm 0.29$ for the formation of $[Fe(\mathbf{1})_2]^{2+}$ (Figure S50). To reverse the process, we added 4-*N*,*N*-dimethylamino-2,2′:6′,2″-terpyridine (**4**) because of its higher affinity for Fe^{2+} ions. After addition of 1 equivalent of **4**, protons a-H and i-H emerged at $\delta = 3.76$ and 8.68 ppm, respectively. Equally, the $N_{azaterpy}$→ZnPor coordination was regained. When a solution of $[Fe(\mathbf{1})_2]^{2+}$ (1×10^{-4} M) in dichloromethane was titrated against **4** (2.5×10^{-3} M), the band at $\lambda = 549$ nm was fully shifted to 562 nm (Figure S32) after addition of one equivalent of **4** (relative to **1**). Quantitative and reversible switching between states IV and III was checked up to two cycles by ^{1}H NMR spectroscopy as well (Figure S12).

After the successful demonstration of reversible toggling between distinct states of nanoswitch **1**, we evaluated the unidirectional cyclic switching along the states IV→I→II→III→IV (Figure S13). As shown above, addition of 1.0 equivalent of copper(I) ions to a solution of switch **1** (state IV) produced the HETTAP complex $[Cu(\mathbf{1})]^+$ (state I). Further addition of 0.50 equivalents of Fe^{2+} ions destroyed the HETTAP complexation and yielded the "dimeric" complex $[Cu_2Fe(\mathbf{1})_2]^{4+}$ (state II). All the spectroscopic data confirm that $[Cu_2Fe(\mathbf{1})_2]^{4+}$ (state II) is equipped with two identical coordinatively frustrated copper(I) complexation sites. Addition of 1.0 equivalent of cyclam (**3**) to $[Cu_2Fe(\mathbf{1})_2]^{4+}$ (relative to **1**) results in the formation of the iron complex $[Fe(\mathbf{1})_2]^{2+}$ (state III). Finally, the Fe^{2+} ions were removed by adding 1.0 equivalent of **4** affording **1** (reset to state IV; for a complete cycle, see Figure S13). In the course of one cycle, $[Cu(\mathbf{3})]^+$ and $[Fe(\mathbf{4})_2]^{2+}$ accumulate as waste products that, however, do not interfere with the switching processes. All the switching processes IV→I→II→III→IV occurred immediately upon mixing the components at room temperature as shown by UV/Vis investigations.[16]

An analysis of the four switching states with their involved stations reveals two options that are suitable for the implementation of catalytic reactions: a) The coordinatively frustrated copper(I) phenanthroline in $[Cu_2Fe(\mathbf{1})_2]^{4+}$ is known for its ability to catalyze click and cyclopropanation reactions. It is exposed only in state II.[10c,e] b) The ZnPor unit is intramolecularly unoccupied in three states (I, II, III), so that a catalytically active species bound to the ZnPor station will be released only in state IV. These considerations suggest that the switching states I and III may serve as OFF states with regard to catalytic activity.

The next step was to select model compounds for a sequential transformation as a proof of concept. Clearly, various interferences could show up that need to be avoided: a) neither the reactant nor the products must intervene in the switching process that links the four switching states, b) the second step of the sequential transformation should selectively only convert the product of the first step, as otherwise side products would form which might intervene in the switching process. Moreover, c) both catalytic processes should work at the same temperature and within the same time. After screening several sequential reactions using a variety of conditions, we finally came up with the optimized substrates **A**, **B**, and **C** shown in Figure 2. The most critical issue was to identify a pair of **A** and **AB** in which only **AB** reacts in the second catalytic process. As the first catalytic step in the cycle $\mathbf{A} + \mathbf{B} \rightarrow \mathbf{AB}$, we selected a click reaction, because we expected it to be catalyzed by the coordinatively frustrated copper(I) phenanthroline available in state II. As **AB** contains the ketotriazole group that could act as a potential chelate complexation unit for metal ions, its binding ability was lowered with the 4-nitrobenzoyl group. In the second step of this cascade, an amine released by state IV should become catalytically active. Actually, an amine such as piperidine (**2**) should be strongly bond to the free ZnPor in all other states (for example, binding of **2** to $[Cu(\mathbf{1})]^+$: $\log K = 5.37 \pm 0.41$, Figure S49), whereas it would hardly bind to **1** ($\log K = 2.66 \pm 0.08$, Figure S47). Consequently, we chose a piperidine-catalyzed Michael-type addition for the process $\mathbf{AB} + \mathbf{C} \rightarrow \mathbf{ABC}$.

Prior to developing the switchable catalysis in presence of **1**, we optimized the conditions for the sequential catalysis in presence of model catalysts. In presence of 10 mol% of $[Cu(\mathbf{5})]^+$ (as a model for $[Cu_2Fe(\mathbf{1})_2]^{4+}$) the click reaction between **A** and **B** (1:1) at 55 °C for 2 h furnished click product **AB** in 54% yield (Figure S33), while in presence of 10 mol% of the HETTAP complex $[Cu(\mathbf{5})(\mathbf{6})]^+$ as a mimic of $[Cu(\mathbf{1})]^+$ no product **AB** was afforded (Figure S34). Secondly, the catalytic reaction between **AB** and Michael acceptor **C** (1:1)

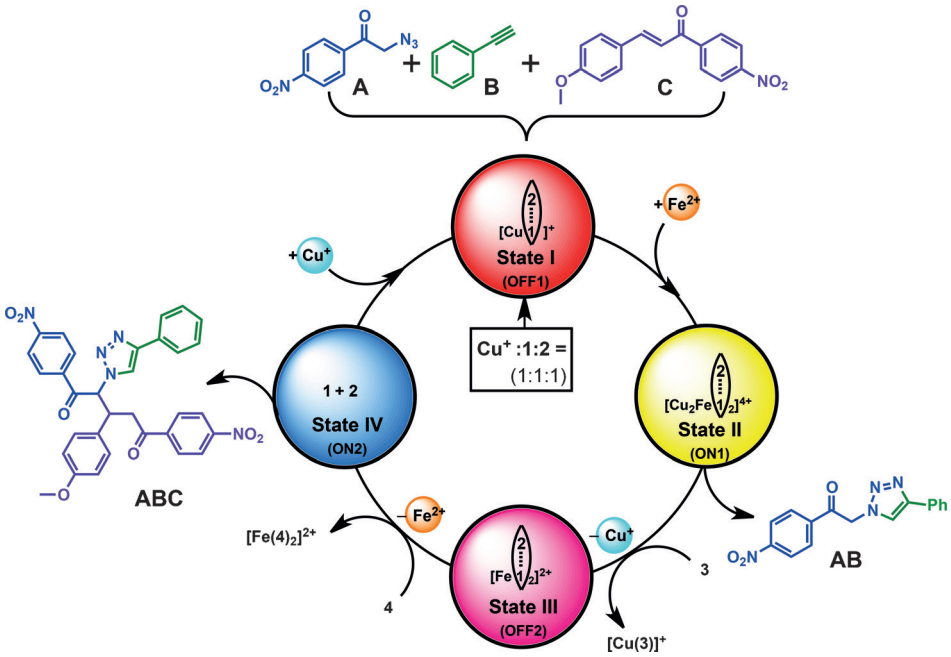

Figure 2. Schematic representation of the switching cycle of nanoswitch **1** with the catalytic transformation of **A** + **B** + **C** → **AB** + **C** → **ABC** occurring in switching states II (ON1) and IV (ON2). For the molecular structures of states I–IV, see Figure 1. Note that in switching states I–III piperidine (**2**) is firmly bound to the ZnPor unit of **1** and thus is not available in solution as a catalytically active species.

in presence of 10 mol% of piperidine provided the Michael addition product **ABC** in 33% yield (Figure S35), while in presence of the piperidine-ZnTPP complex[17] the product **ABC** did not arise (Figure S42).

After the successful implementation of sequential catalysis, the ability of the eleven-component-system (nanoswitch **1**, piperidine (**2**), the four inputs for switching, reactants **A** + **B** + **C**, and products **AB** + **ABC**) to function in a one-pot process was tested in two consecutive switching cycles. For this purpose (^{1}H NMR data for the 1st cycle, Figure S45 a–d), an NMR tube containing $[Cu(\mathbf{1})]^+$ (1.97 mM), piperidine (**2**), **A**, **B**, and **C** in a 1:1:10:10:10 ratio in $CDCl_3$ was heated to 55 °C for 2 h. By NMR spectroscopy, no product formation was found (catalysis OFF1 in state I, see Figure 3 a), which is readily rationalized on the basis that piperidine (**2**) is firmly bound to the ZnPor site of $[Cu(\mathbf{1})(\mathbf{2})]^+$ and copper(I) is buried in the HETTAP complexation site. Addition of 0.50 equivalents of Fe^{2+} ions transformed $[Cu(\mathbf{1})(\mathbf{2})]^+$ to $[Cu_2Fe(\mathbf{1})_2(\mathbf{2})_2]^{4+}$ (state II, Figure 2). Heating at 55 °C for 2 h afforded the click reaction product **AB** in 50% yield (Figure 3 b),[18] while no Michael addition product was detected (catalysis ON1 in state II). Notably, the catalytic activity of $[Cu_2Fe(\mathbf{1})_2(\mathbf{2})_2]^{4+}$ was almost the same as that seen in the model reaction in the presence of $[Cu(\mathbf{5})]^+$. After addition of one equivalent (relative to **1**) of cyclam (**3**) to remove the Cu^+ ions from phenanthroline binding site, the complex $[Fe(\mathbf{1})_2(\mathbf{2})]^{2+}$ (state III) was afforded. As expected, heating at 55 °C for 2 h did not produce any further click reaction product **AB** (total yield of **AB** = 50%, see Figure 3 c). Moreover, no Michael addition product was detected in the NMR spectrum, attesting a complete shutdown of both catalytic reactions (catalysis OFF2 in state III). Now 1.0 equivalent of 4-*N*,*N*-dimethylamino-2,2′:6′,2″-terpyridine (**4**) was added to trap the Fe^{2+} ions and to generate the nanoswitch **1** (state IV). At this point, the switching arm moved to the ZnPor station, which consequently should release piperidine (**2**). Indeed, the heating of state IV at 55 °C for 2 h afforded the Michael addition product **ABC** in 14% absolute yield (28% yield relative to **AB**, Figures 3 d and Figure S45). The reactant for the Michael addition step, **AB**, is used up consistently (−26%; catalysis ON2 in state IV). Then, the second cycle was started after replacing the used-up reactants **A** + **B** to create identical starting conditions as for the first cycle (^{1}H NMR data for 2nd cycle, Figure S46 e-i). After addition of one equivalent of Cu^+ ions and the generation of $[Cu(\mathbf{1})(\mathbf{2})]^+$ (state I), the product yields

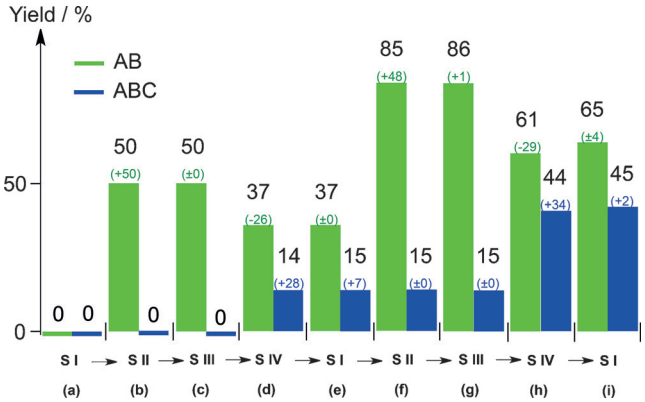

Figure 3. Evolution of the yield (black numbers) of **AB** and **ABC** in the various switching states (S = State) over the course of two cycles. The yields (or losses) for each step are given in brackets (%) with regard to the quantity (or consumed amount) of the starting material.

remained almost unaltered after a repeated heating at 55 °C for 2 h (click product **AB** = 37%, Michael addition product **ABC** = 15%, Figure 3 e), which corresponds to OFF1. Addition of 0.50 equivalents of Fe^{2+} ions and heating of the mixture (state II) at 55 °C for 2 h furnished the click product **AB** in 48% yield (Figure 3 f: 85% is the total yield in the 2nd cycle with regard to one equivalent of **A**). At the same time, no additional Michael addition product **ABC** was afforded (ON1). Trapping of Cu^+ ions by 1.0 equivalent of cyclam and subsequent heating under similar conditions turned off both reactions (OFF2; Figure 3 g). The addition of 1.0 equivalent of **4** restored compound **1**. Now heating at 55 °C for 2 h

afforded the Michael addition product **ABC** in 44% absolute yield, which corresponds to a 34% conversion in the 2nd cycle (Figures 3h and Figure S46).[19] Finally, the addition of one equivalent of Cu^{+} ions turned off both catalyses (OFF1; Figure 3i).

Both, the formation of the two catalytically generated products and the mass balance of all steps are remarkably reproducible over two cycles. In both cycles the conversion of **A** + **B** → **AB** is 50% (see Figure 3b,f; relative to **A**), while that of **AB** → **ABC** is 28% and 34% (relative to consumed **AB**).[19] Furthermore, the consumption of **AB** (−26 and −29%) corresponds in both cycles to the production of **ABC** (+28 and +34%) within the errors of integration. These yields are in addition very close to those of the model reactions furnishing click product **AB** in 54% yield (using $[Cu(\mathbf{5})]^{+}$) and the Michael addition product **ABC** in 33% yield (using piperidine). Thus, all features demonstrate a remarkable reproducibility in the twice repeated cyclic ON/OFF switching of an eleven-component reaction system. A third cycle was hampered by the partial precipitation of **ABC** from the reaction mixture.

Switchable catalysis is no end in itself. As recently highlighted by Leigh et al.,[5b] it is a key challenge to switch several subsequent processes by a distinct sequence of stimuli. With the system presented herein, the first four-state nanoswitch,[14] we demonstrate that a two-step sequential catalysis can be commanded with high reproducibility over the course of two full cycles. This performance has to be valued as considerably higher than that of systems with only two switching states, in which the activity of both catalytic species is not exclusively controlled by the switch.[10e] Even though the complexity of the pyruvate dehydrogenase complex[20] with its three interacting enzymes will certainly not be reached, two cascading catalytic processes are toggled in an interwoven eleven-component reaction system without any interferences (see Figure 2). Thus, the present work enlarges our fundamental understanding of how to network complex reaction scenarios under system control and free from interference.[21]

Acknowledgements

We are grateful to the DAAD (Deutscher Akademischer Austauschdienst), the DFG Deutsche Forschungsgemeinschaft (Schm-647/19-1), and the Universität Siegen for financial support.

Keywords: allosteric control · coordination chemistry · molecular switches · nanomechanical motion · sequential catalysis

How to cite: *Angew. Chem. Int. Ed.* **2016**, *55*, 10512–10517
Angew. Chem. **2016**, *128*, 10668–10673

[1] D. P. Giedroc, A. I. Arunkumar, *Dalton Trans.* **2007**, 3107–3120.
[2] K. J. Waldron, N. J. Robinson, *Nat. Rev. Microbiol.* **2009**, *7*, 25–35.
[3] a) B. Champin, P. Mobian, J.-P. Sauvage, *Chem. Soc. Rev.* **2007**, *36*, 358–366; b) M. J. Wiester, P. A. Ulmann, C. A. Mirkin, *Angew. Chem. Int. Ed.* **2011**, *50*, 114–137; *Angew. Chem.* **2011**, *123*, 118–142; c) U. Lüning, *Angew. Chem. Int. Ed.* **2012**, *51*, 8163–8165; *Angew. Chem.* **2012**, *124*, 8285–8287; d) N. Kumagai, M. Shibasaki, *Catal. Sci. Technol.* **2013**, *3*, 41–57; e) X. Su, I. Aprahamian, *Chem. Soc. Rev.* **2014**, *43*, 1963–1981; f) P. Ceroni, A. Credi, M. Venturi, *Chem. Soc. Rev.* **2014**, *43*, 4068–4083; g) S. Erbas-Cakmak, D. A. Leigh, C. T. McTernan, A. L. Nussbaumer, *Chem. Rev.* **2015**, *115*, 10081–10206; h) A. J. McConnell, C. S. Wood, P. P. Neelakandan, J. R. Nitschke, *Chem. Rev.* **2015**, *115*, 7729–7793; i) P. C. Knipe, S. Thompson, A. D. Hamilton, *Chem. Sci.* **2015**, *6*, 1630–1639.
[4] C. Kremer, A. Lützen, *Chem. Eur. J.* **2013**, *19*, 6162–6196.
[5] a) M. Raynal, P. Ballester, A. Vidal-Ferran, P. W. N. M. van Leeuwen, *Chem. Soc. Rev.* **2014**, *43*, 1734–1787; b) V. Blanco, D. A. Leigh, V. Marcos, *Chem. Soc. Rev.* **2015**, *44*, 5341–5370; c) M. Schmittel, *Chem. Commun.* **2015**, *51*, 14956–14968.
[6] a) F. Würthner, J. Rebek, Jr., *Angew. Chem. Int. Ed. Engl.* **1995**, *34*, 446–448; *Angew. Chem.* **1995**, *107*, 503–505; b) H. Sugimoto, T. Kimura, S. Inoue, *J. Am. Chem. Soc.* **1999**, *121*, 2325–2326; c) R. Cacciapaglia, S. Di Stefano, L. Mandolini, *J. Am. Chem. Soc.* **2003**, *125*, 2224–2227; d) M. V. Peters, R. S. Stoll, A. Kühn, S. Hecht, *Angew. Chem. Int. Ed.* **2008**, *47*, 5968–5972; *Angew. Chem.* **2008**, *120*, 6056–6060; e) R. S. Stoll, S. Hecht, *Angew. Chem. Int. Ed.* **2010**, *49*, 5054–5075; *Angew. Chem.* **2010**, *122*, 5176–5200; f) J. Wang, B. L. Feringa, *Science* **2011**, *331*, 1429–1432; g) O. B. Berryman, A. C. Sather, A. Lledó, J. Rebek, Jr., *Angew. Chem. Int. Ed.* **2011**, *50*, 9400–9403; *Angew. Chem.* **2011**, *123*, 9572–9575; h) B. M. Neilson, C. W. Bielawski, *J. Am. Chem. Soc.* **2012**, *134*, 12693–12699; i) B. M. Neilson, C. W. Bielawski, *ACS Catal.* **2013**, *3*, 1874–1885; j) B. M. Neilson, C. W. Bielawski, *Chem. Commun.* **2013**, *49*, 5453–5455; k) B. M. Neilson, C. W. Bielawski, *Organometallics* **2013**, *32*, 3121–3128; l) L. Osorio-Planes, C. Rodríguez-Escrich, M. A. Pericàs, *Org. Lett.* **2014**, *16*, 1704–1707.
[7] a) V. Blanco, A. Carlone, K. D. Hänni, D. A. Leigh, B. Lewandowski, *Angew. Chem. Int. Ed.* **2012**, *51*, 5166–5169; *Angew. Chem.* **2012**, *124*, 5256–5259; b) V. Blanco, D. A. Leigh, V. Marcos, J. A. Morales-Serna, A. L. Nussbaumer, *J. Am. Chem. Soc.* **2014**, *136*, 4905–4908; c) J. Beswick, V. Blanco, G. De Bo, D. A. Leigh, U. Lewandowska, B. Lewandowski, K. Mishiro, *Chem. Sci.* **2015**, *6*, 140–143; d) C. M. Álvarez, H. Barbero, D. Miguel, *Eur. J. Org. Chem.* **2015**, 6631–6640.
[8] a) H. J. Yoon, J. Kuwabara, J.-H. Kim, C. A. Mirkin, *Science* **2010**, *330*, 66–69; b) C. M. McGuirk, C. L. Stern, C. A. Mirkin, *J. Am. Chem. Soc.* **2014**, *136*, 4689–4696.
[9] a) I. O. Fritsky, R. Ott, R. Krämer, *Angew. Chem. Int. Ed.* **2000**, *39*, 3255–3258; *Angew. Chem.* **2000**, *112*, 3403–3406; b) M. Galli, J. E. M. Lewis, S. M. Goldup, *Angew. Chem. Int. Ed.* **2015**, *54*, 13545–13549; *Angew. Chem.* **2015**, *127*, 13749–13753.
[10] a) M. Schmittel, S. De, S. Pramanik, *Angew. Chem. Int. Ed.* **2012**, *51*, 3832–3836; *Angew. Chem.* **2012**, *124*, 3898–3902; b) M. Schmittel, S. Pramanik, S. De, *Chem. Commun.* **2012**, *48*, 11730–11732; c) S. De, S. Pramanik, M. Schmittel, *Dalton Trans.* **2014**, *43*, 10977–10982; d) G.-H. Ouyang, Y.-M. He, Y. Li, J.-F. Xiang, Q.-H. Fan, *Angew. Chem. Int. Ed.* **2015**, *54*, 4334–4337; *Angew. Chem.* **2015**, *127*, 4408–4411; e) S. De, S. Pramanik, M. Schmittel, *Angew. Chem. Int. Ed.* **2014**, *53*, 14255–14259; *Angew. Chem.* **2014**, *126*, 14480–14484.
[11] S. Venkataramani, U. Jana, M. Dommaschk, F. D. Sönnichsen, F. Tuczek, R. Herges, *Science* **2011**, *331*, 445–448.
[12] a) D. Ray, J. T. Foy, R. P. Hughes, I. Aprahamian, *Nat. Chem.* **2012**, *4*, 757–762; b) S. Pramanik, S. De, M. Schmittel, *Angew. Chem. Int. Ed.* **2014**, *53*, 4709–4713; *Angew. Chem.* **2014**, *126*, 4798–4803; c) S. Pramanik, S. De, M. Schmittel, *Chem.*

Commun. **2014**, *50*, 13254 – 13257; d) Y. Ren, L. You, *J. Am. Chem. Soc.* **2015**, *137*, 14220 – 14228.
[13] a) R. N. Perham, *Annu. Rev. Biochem.* **2000**, *69*, 961 – 1004; b) N. Mast, A. J. Annalora, D. T. Lodowski, K. Palczewski, C. D. Stout, I. A. Pikuleva, *J. Biol. Chem.* **2011**, *286*, 5607 – 5613; c) P. F. Leadlay, *Nature* **2014**, *510*, 482 – 483.
[14] Three-State Switch: G. Fioravanti, N. Haraszkiewicz, E. R. Kay, S. M. Mendoza, C. Bruno, M. Marcaccio, P. G. Wiering, F. Paolucci, P. Rudolf, A. M. Brouwer, D. A. Leigh, *J. Am. Chem. Soc.* **2008**, *130*, 2593 – 2601.
[15] M. L. Saha, S. Neogi, M. Schmittel, *Dalton Trans.* **2014**, *43*, 3815 – 3834.
[16] To obtain reliable kinetic data, stopped-flow investigations would be warranted.
[17] ZnTPP = zinc(II) 5,10,15,20-tetraphenylporphyrin.
[18] The yield of products **AB** and **ABC** was determined with respect to the internal standard **7** using integration of the ^{1}H NMR spectra.
[19] The slightly higher yield of **ABC** is rationalized due to the higher concentration of **AB** in the second cycle.
[20] M. S. Patel, T. E. Roche, *FASEB J.* **1990**, *4*, 3224 – 3233.
[21] J. Li, P. Nowak, S. Otto, *J. Am. Chem. Soc.* **2013**, *135*, 9222 – 9239.

Received: May 12, 2016
Published online: July 20, 2016

